DIFFERENTIAL-CROSS-MULTIPLIER DEMODULATION OF INTERFEROMETRIC OPTICAL FIBER SENSORS

by C.C. Chang and J.S. Sirkis

In recent years optical fiber sensors have seen increasing transition from the development phase to field applications. This transition has been somewhat inhibited by the lack of commercial vendors that can provide the instrumentation required to interpret the optical signals produced by the sensors. This problem is compounded by the fact that it is generally mechanical civil, or aerospace engineers who want to apply this technology, and these disciplines generally view the development of electronic circuitry with a certain level of intimidation. This paper is the second in a series of tutorials that are intended to enhance the proliferation of optical fiber sensors in the experimental mechanics community by concentrating on the differential-cross-multiplier sensor demodulation technique. Effort is expended to explain the demodulation philosophy, provide electrical circuits, and to explain adjustment procedures. Ref. 2 details provides a similar discussion of active homodyne demodulation.

CONCEPTS AND MATHEMATICAL DEVELOPMENT

The phase generate carrier (PGC) demodulation technique described in this paper can be decomposed into two principal components. The first is creating electric signals that are proportional to $\sin(\phi(t))$ and $\cos(\phi(t))$, where $\phi(t)$ is the time varying, load induced phase change experienced by an interferometric optical fiber sensor. The second component of the demodulation technique extracts the unambiguous phase change, $\phi(t)$ from $\sin(\phi(t))$ and $\cos(\phi(t))$. The $\sin(\phi)$ and $\cos(\phi)$ can be obtained from an interferometric signal by applying a cosinusoidal phase carrier either by modulating the laser frequency[1] or by using a piezoelectric (usually PZT cylinder) stretching device to one arm of a two arm fiber interferometer.[1,2] Laser frequency modulation is commonly used with diode lasers since their frequency is proportional to their driving current. On the other hand, PZT cylinders are generally used when diode lasers are not available, which will most likely be the case for researchers just beginning efforts in optical fiber sensor applications. This paper will assume that the latter phase modulation technique is used, although demodulation technique described in this paper works equally well the laser frequency modulation. Consider the general form for the intensity exiting an optical fiber interferometer that is experiencing cosinusoidal phase modulation,

$$I = A + B\cos(\phi_c\cos(\omega_c t) + \phi(t)); \tag{1}$$

where $\phi_c\cos(\omega_c t)$ is the PGC signal, with ϕ_c being the *depth of modulation* and ω_c being the *carrier frequency*. Equation (1) can be expanded in a series of Bessel functions[1] to produce

$$I = A + B\left\{\left[J_0(\phi_c) + \sum_{k=1}^{\infty}(-1)^k J_{2k}(\phi_c)\cos(2k\omega_c t)\right]\cos(\phi(t)) - \left[2\sum_{k=0}^{\infty}(-1)^k J_{2k+1}(\phi_c)\cos((2k+1)\omega_c t)\right]\sin(\phi(t))\right\}. \tag{2}$$

If this equation is multiplied by $\cos(\omega_c t)$, the trigonometric identity $\cos^2(\omega_c t) = 1/2(1 + \cos(2\omega_c t))$ is used, and then a low pass filter is used to eliminate all components associated with the carrier, then all that is left is

$$I_s = BJ_1(\phi_c)\sin(\phi(t)). \tag{3}$$

Similarly, multiplying eq (2) by $\cos(2\omega_c t)$ and low pass filtering yields

$$I_c = -BJ_2(\phi_c)\cos(\phi(t)). \tag{4}$$

Equations (1) through (4) show that it is possible to obtain signals that are proportional to the sine and cosine of the load induced phase change, $\phi(t)$.

The next step in the phase demodulation is the extract of $\phi(t)$ from eqs (3) and (4). This can be accomplished by using the DCM approach by which I_s is differentiated and multiplied by I_c, then subtracted from I_s multiplied by the derivative of I_c. This process is stated mathematically as

$$Z = I_c\frac{dI_s}{dt} - I_s\frac{dI_c}{dt}. \tag{5}$$

Upon substitution of eqs. (3) and (4) into eq. (5) and then integrating, one finds that the load induced phase is given by

$$\phi(t) = \int_0^t Z dt. \tag{6}$$

Like eqs (3) and (4), the eqs (5) and (6) can be easily implemented electronically with analog differentiator, multiplier, difference amplifier and integrator circuits. A more detailed mathematical development of this demodulation scheme can be found in Ref. 1.

EXPERIMENTAL ARRANGEMENT

The purpose of this paper is to detail optical fiber sensor demodulation using the differential-cross-multiplier demodulation technique. Therefore the complexity in the fiber optic sensor configurations and modulation technique used in this demonstration is purposely kept to a minimum. This demonstration arrangement is shown in Fig. 1 and is known as a Michelson sensor.[3] Light from a HeNe laser is launched into a single mode (λ_c = 600 nm) 2 × 2 coupler which separates the light into the reference and sensing fibers. Both the reference and sensing fibers are cleaved and have a thin film of aluminum sputtered onto their ends to act as mirrors in order to reflect the light back towards the coupler. Three or more coatings are generally required in standard sputtering (or vacuum deposition) chambers in order to achieve high reflectivity. Roughly ten meters of the reference fiber is

C.C. Chang is a Graduate Research Assistant, and J.S. Sirkis (SEM Member) is Associate Professor, Smart Materials and Structure Research Center, Department of Mechanical Engineering, University of Maryland, College Park, MD.

wrapped around a PZT cylinder for use as a phase modulator. As mentioned earlier, phase modulation can be achieved via modulating the driving current of a diode laser, but the PZT technique can be implemented with gas lasers that are commonly available at research facilities. The sensing fiber must include a fiber coil (not exposed to the load field) that is roughly equal to that wrapped around the PZT cylinder in order to maintain the optical path difference of the Michelson interferometer within the coherence length of the laser source.

The light from the reference and sensing fibers mix at the 2 × 2 coupler to form coherent interference that is recorded by the photodetector (*ν*-Physics Mo. 2001). If a carrier signal is applied to the PZT cylinder as indicated in Fig. 1, then the photodetector current will have the form specified in eq (1). The carrier signal is also provided to the DCM demodulator in order to perform the multiplications that lead to eqs (3) and (4). Block diagrams of the two primary components of the DCM demodulator are shown in Figs. 2a and 2b. Fig. 2a schematically depicts the carrier signal (from the function generator in Fig. (1)) and the photodetector signal being passed to the demodulator, where the carrier is phase shifted and then split into three leads. The first two are self-multiplied to obtain $\cos(\omega_c t)$ which is then multiplied by the photodetector signal (eq (1)) and amplified. This signal is then low-pass filtered and amplified again to yield a signal proportional to $\cos(\phi(t))$ (eq (3)). The third leg of the carrier is multiplied by the photodetector signal, low-pass filtered, and amplified to yield a signal proportional to $\sin(\phi(t))$ (eq (4)).

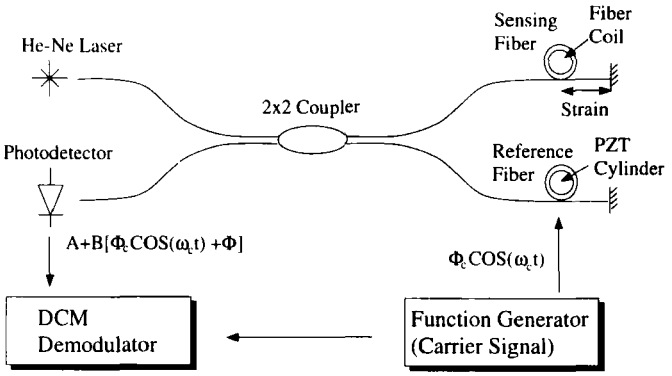

Fig. 1—*Optical fiber sensor demodulation*

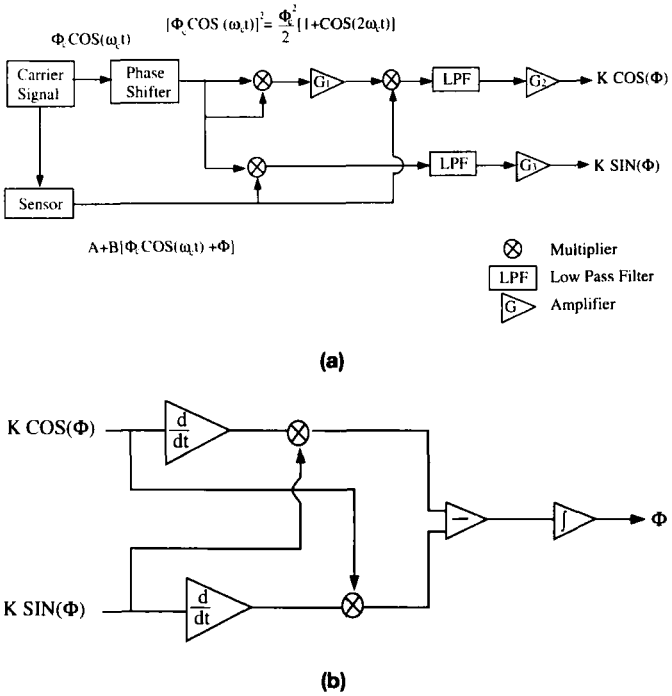

Fig. 2—*(a) block diagram of electronics used to create sin(ϕ(t)) and cos(ϕ(t)), (b) block diagram of differential-cross-multiplier*

The phase shifter is included to account for phase-delays caused by subsequent electronics, and the amplifier between the two multipliers in the $\cos(\phi(t))$ path is used to make the amplitudes of the $\cos_2(\omega_c t)$ and $\cos(\omega_c t)$ signals have roughly the same. The amplifiers after both low pass filters are used to make the amplitudes of the $\sin(\phi(t))$ and $\cos(\phi(t))$ equal. The second segment of the demodulator (Fig. 2b) performs the differentiation, cross-multiplication, subtraction, and integration as indicated in eqs (5) and (6).

The block diagrams in Fig. 2 can be implemented using analog electronics by cascading relatively simple electronic circuits. Figure 3 shows a complete circuit diagram of a DCM demodulator designed for a 40 KHz carrier signal. The top of this circuit diagram generally corresponds to Fig. 2a while the bottom generally corresponds to Fig. 2b. Note also that this diagram has replaced the function generator with an on-board (DATEL ROJ-1K) sine-wave oscillator (A in Fig. 3) and an amplifier (C in Fig. 3). This amplifier is used to adjust the amplitude (depth of modulation) of the carrier signal (ϕ_c in eqs 1 and 2). These two components can be removed if an external function generator is used, in which case the function generator signal passes through the phase shifter (B in Fig. 3) and proceeds to the multipliers. Multiplication is accomplished with ANALOG DEVICES AD534 analog multiplier chips, although a variety of such chips are available. The multiplier labeled D in Figure 3 multiplies the carrier signal by the photodetector signal, then sends the result to a fifth order Butterworth low pass filter (H in Fig. 3) that has been designed to have a cutoff frequency of 6 KHz. This signal then passes through the final gain stage (J in Fig. 3) to yield $\sin(\phi(t))$. The phase shifted carrier signal is also provided to the multiplier labeled E in Fig. 3, which squares the carrier. The result is amplified (F in Fig. 3) and then multiplied by the photodetector signal (G in Fig. 3), low pass filtered (I in Fig. 3) and amplified again (K in Fig. 3) to yield $\cos(\phi(t))$. The $\sin(\phi(t))$ and $\cos(\phi(t))$ signals are then differentiated (L in Fig. 3), cross-multiplied (M in Fig. 3), subtracted (N in Fig. 3), and integrated (O in Fig. 3). With the exception to the oscillator and the multipliers, all electronic operations are performed using standard operational amplifiers (OP-AMPs). The AD844 OP-AMP is used for the phase shifter labeled B and the amplifier labeled C and F in Fig. 3 because this particular OP-AMP has a high frequency response. The frequency response of the other components was not a consideration in OP-AMP choice for this circuit. For details of the individual circuits used to develop the DCM demodulator shown in Fig. 3, the reader should see Refs. 4–6 or equivalents.

The circuit diagram in Fig. 3 has numerous adjustment potentiometers (pots), it is therefore worthwhile to outline an adjustment procedure. Firstly, the depth of modulation of the carrier should be adjusted so that $J_1(\phi_c) = J_2(\phi_c)$. This reduces the dependence of the demodulator on any variations in ϕ_c, and can be easily accomplished by viewing the photodetector signal on an oscilloscope and adjusting the depth of modulation until the trace resembles the trace in Fig. 4a. Note that the depth of modulation is related to the voltage applied to the PZT cylinder in Fig. 1, as well as to the amount of figure wrapped around the PZT cylinder. Next, the amplifier labeled F in Fig. 3 should be adjusted so that the amplitudes of $\cos_2(\omega_c t)$ and $\cos(\omega_c t)$ are roughly equal, and equal to the amplitude of the photodetector signal. The output voltage of the multipliers (and OP-AMPs for

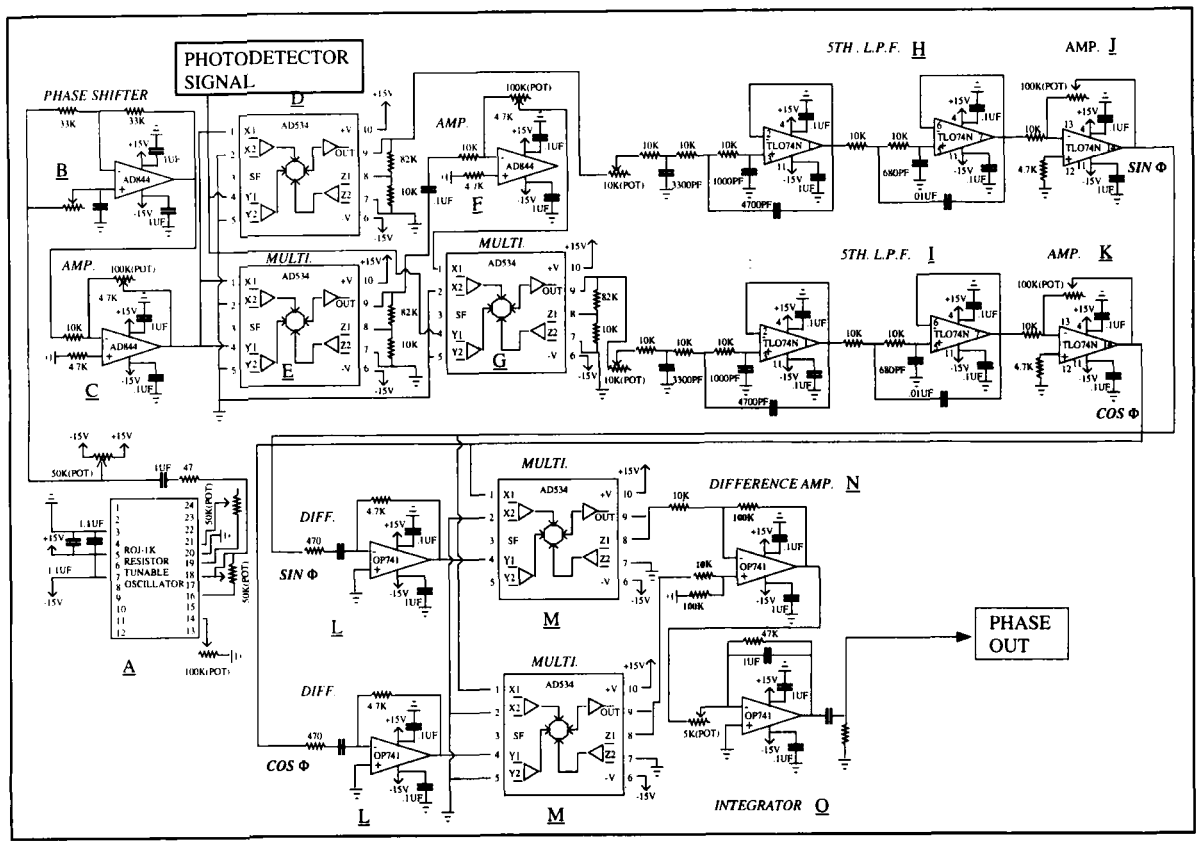

Fig. 3—*The circuit diagram of the electronic DCM demodulator*

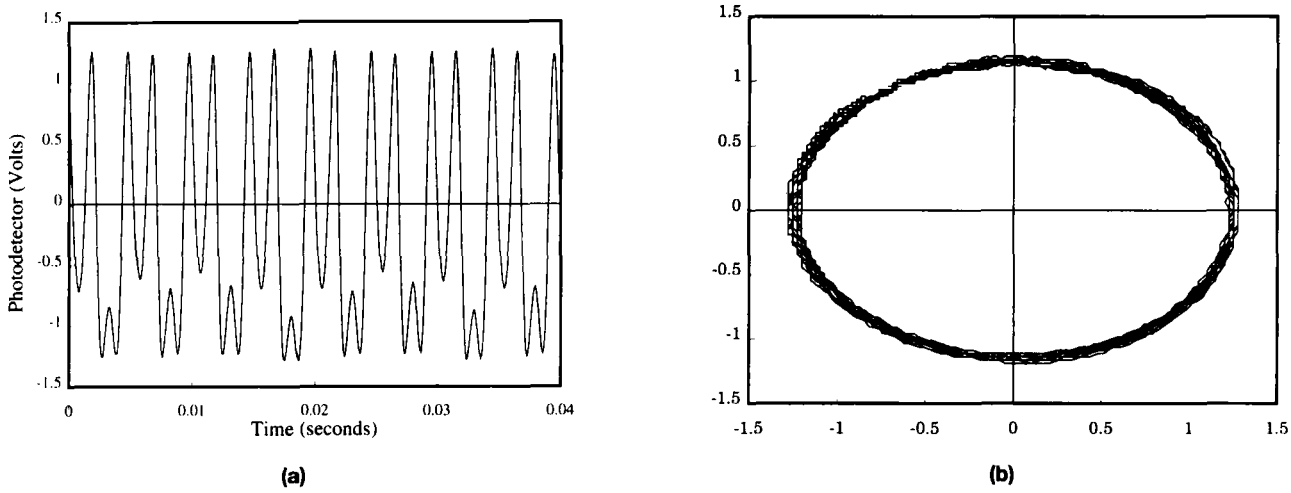

Fig. 4—*(a) The photodetector signal, (b) X-Y plot of sin(ϕ(t)) versus cos(ϕ(t))*

that matter) are limited to the voltage levels used to power the chips (+/− 15 V in this case). A signal exceeding this level will be distorted in some way (generally clipped). As a result, care must be taken to keep the voltage levels of the carrier to a level low enough that the squaring operation performed by multiplier G does not clip the output signal. This is a common source of difficulty, and is usually solved by adjusting the gain on the detector electronics. In the final adjustments, the phase shifter and amplifiers labeled J and K are adjusted so that $\sin(\phi(t))$ and $\cos(\phi(t))$ are in phase and have equal amplitude. The best way to perform this adjustment is to display $\sin(\phi(t))$ and $\cos(\phi(t))$ on an oscilloscope in a cross-plot using the X-Y option on the time-division selector. An in-phase and equal amplitude $\sin(\phi(t))$ and $\cos(\phi(t))$ will appear as a circle on the oscilloscope screen when load is being applied to the sensor. Figure 4b shows a cross-plot of $\sin(\phi(t))$ and $\cos(\phi(t))$ for a $+/-\pi$ phase shift applied to the sensing arm of the interferometer. This cross-plot is elliptical because the amplitudes of $\sin(\phi(t))$ and $\cos(\phi(t))$ are not equal. The remaining adjustment pots in Fig. 3 are used to make slight adjustments to the gain or cutoff characteristics of the various components, and are usually not changed after they are set initially. Finally, if a carrier other than 40 KHz is desired, one only has to 1) set the cutoff of the low pass filters to eliminate the higher order harmonics, and 2) make sure that the circuit has sufficient frequency response to operate at higher frequencies. The circuit given in Fig. 3 can operate at carrier

frequencies ranging from 30 KHz to 60 KHz without modification.

RESULTS

An aluminum beam vibration test was performed to verify the differential-cross-multiplier demodulation technique for optical fiber sensors. The sensing fiber with a gage length of 3.5 in was taped onto the cantilever beam which has dimensions of 8.5 in by 1 in. Because the output signal from the DCM demodulator was in voltages, a calibration factor is required to convert voltage output to phase shift. A simple way to obtain the factor is to glue a 2 in gage length of sensing fiber onto a PZT5H plate which has dimensions of 2 in by 1 in, and then a sinusoidal strain generated from the PZT plate can be controlled by a function generator. A full circle from the X-Y plot on an oscilloscope similar to Fig. 4a can be obtained by adjusting the amplitude of the function generator. This full circle represents a phase shift of 2π corresponded to a fixed output voltage from the DCM demodulator. Thus, the ratio can be used as the calibration factor to convert voltage signals to phase shift. The beam vibration test through the DCM demodulator was shown in Fig. 5, which has a frequency around 50 Hz.

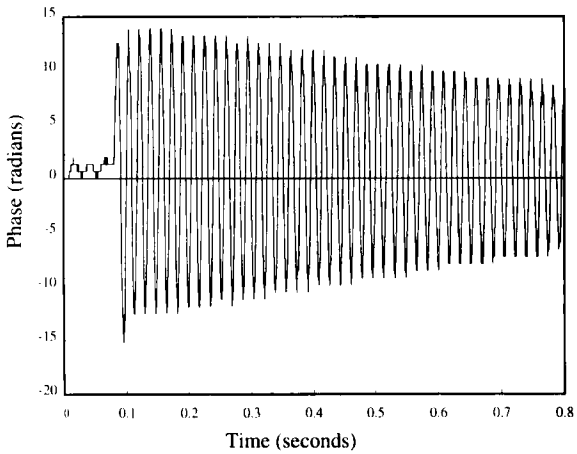

Fig. 5—*DCM Signal for Aluminum Beam under Free Vibration*

CONCLUSIONS

This paper details the differential-cross-multiplier demodulation technique for optical fiber sensors in an attempt to help proliferate the use of optical fiber sensors by the experimental mechanics community. This demodulation technique is widely used by the fiber sensors community with a wide variety of interferometric optical fiber sensor configurations. An effort has been made to provide sufficient detail in the concepts of operation, circuitry, and requisite adjustments to enable even a novice to implement this demodulation scheme.

REFERENCES

1. Dandridge, A., Tveten, A.B., and Giallorenzi, T.G., "Homodyne Demodulation Scheme for Fiber Optics Sensors using Phase Generated Carrier," IEEE Jou. Quan. Elect., **QE-18***(10), 1647–1653.*

2. Lo, Y.L., and Sirkis, J.S., "Active Homodyne Demodulation of Mach-Zehnder Interferometric Optical Fiber Sensors," to appear in EXPERIMENTAL TECHNIQUES.

3. Dalley, J.W., Riley, W.F., and Sirkis, J.S., "Strain Gages," in the Handbook on Experimental Mechanics, 2nd Edition A.S. Kobayashi, Ed., VCH Publ., NY, 1993.

4. Franco, S., Design with Operational Amplifiers and Analog Integrated Circuits, McGraw-Hill, NY (1988).

5. Choudhury, D.R., and Jain, S., Linear Integrated Circuits, John Wiley and Sons, NY (1991).

6. Markus, J., and Weston, C., Essential Circuits Reference Guide, McGraw-Hill, NY (1988).